Acta Crystallographica Section A
Foundations of Crystallography
ISSN 0108-7673

Received 20 April 2000
Accepted 17 July 2000

The statistical kinematical theory of X-ray diffraction as applied to reciprocal-space mapping

Yakov I. Nesterets[a]* and Vasily I. Punegov[b]

[a]Department of Theoretical and Computing Physics, Syktyvkar State University, Oktyabrskii pr. 55, 167001 Syktyvkar, Russia, and [b]Department of Solid State Physics, Syktyvkar State University, Oktyabrskii pr. 55, 167001 Syktyvkar, Russia. Correspondence e-mail: nester@ssu.komi.com

The statistical kinematical X-ray diffraction theory is developed to describe reciprocal-space maps (RSMs) from deformed crystals with defects of the structure. The general solutions for coherent and diffuse components of the scattered intensity in reciprocal space are derived. As an example, the explicit expressions for intensity distributions in the case of spherical defects and of a mosaic crystal were obtained. The theory takes into account the instrumental function of the triple-crystal diffractometer and can therefore be used for experimental data analysis.

1. Introduction

Triple-crystal diffractometry is widely used for the analysis of the structural characteristics of monocrystals and heteroepitaxic systems (Iida & Kohra, 1979; Zaumseil & Winter, 1982*a*,*b*; Lomov *et al.*, 1985). At present, X-ray reciprocal-space mapping (RSM) is a very promising method for such investigations (Faleev *et al.*, 1999).

Various versions of the kinematical theory have been used for an evaluation of the scattered intensity around a reciprocal-lattice node. Holý *et al.* (1994) have applied a formalism based on the mutual coherence function to investigate the defects in epitaxic layers. The modified Krivoglaz (1996) kinematical approach is used by Kaganer *et al.* (1997) for evaluation of diffusely scattered intensity in a reciprocal space from heteroepitaxic structures with misfit dislocations.

Using the statistical dynamical diffraction formalism (Kato, 1980*a*,*b*; Pavlov & Punegov, 1998*a*,*b*), we have developed the theory for the case of so-called triple-crystal diffractometry (Pavlov & Punegov, 2000). The general expressions for coherently and diffusely scattered intensity in reciprocal space are obtained. In this theory, instead of Kato's correlation length τ (the case of a spherical incident wave) (Kato, 1980*a*,*b*) or Bushuev's correlation length $\tau(\omega)$ (Bushuev, 1989) (the case of a plane incident wave in double-crystal diffractometry), a correlation area $\tau(\omega,\varepsilon)$ is introduced, where ω is the angular deviation of the sample, ε is the angular deviation of the crystal analyzer. Though the theory (Pavlov & Punegov, 2000) is most general and may be applied for crystals of any thickness, however, expressions for coherently and diffusely scattered intensities are very complicated for practical use.

The experimental intensity distributions in reciprocal space contain both coherent and diffuse components (Faleev *et al.*, 1999). Meanwhile, in most cases, either pure diffuse scattering (Holý *et al.*, 1994; Kaganer *et al.*, 1997) or coherent scattering solely (Pavlov *et al.*, 1999) is taken into account. The simultaneous account of coherent and diffuse components of the scattered intensity allows one to obtain the most complete information about the structure under investigation (Holý *et al.*, 1995; Darhuber *et al.*, 1997).

The aim of this paper is to develop the statistical kinematical theory applied to triple-crystal diffractometry taking into account charge density and interplanar spacing variations. The influence of the instrumental function of the triple-crystal diffractometer on formation of a RSM is discussed.

2. Basic equations

Let us assume the plane monochromatic X-ray wave to be incident on a crystal surface that coincides with the XY plane and the plane of diffraction with the XZ plane of the Cartesian coordinates system (see Fig. 1). In the kinematical diffraction theory, which neglects the multiple rescattering of the waves, the amplitudes of transmitted and reflected waves are found from the following system of equations:

$$\begin{aligned}\left(\cot\theta_1\frac{\partial}{\partial x}+\frac{\partial}{\partial z}\right)E_0(\mathbf{r}) &= i\sigma_0(\mathbf{r})E_0(\mathbf{r})\\ \left(\cot\theta_2\frac{\partial}{\partial x}-\frac{\partial}{\partial z}\right)E_h(\mathbf{r}) &= i[b\sigma_0(\mathbf{r})+\eta]E_h(\mathbf{r})\\ &\quad + i\sigma_h(\mathbf{r})\exp[-i\mathbf{hu}(\mathbf{r})]E_0(\mathbf{r}),\end{aligned} \tag{1}$$

where

$$\sigma_0(\mathbf{r})=\pi\chi_0(\mathbf{r})/\lambda\gamma_0,\quad \sigma_h(\mathbf{r})=\pi\chi_h(\mathbf{r})C/\lambda\gamma_h,$$
$$\eta=2\pi\omega\sin(2\theta_B)/\lambda\gamma_h,\quad \gamma_{0,h}=\sin\theta_{1,2},\quad b=\gamma_0/\gamma_h.$$

Here λ is the X-ray wavelength, θ_B the kinematical Bragg angle of the diffracting planes with the reciprocal-space vector $\mathbf{h}$, C the polarization factor, $\chi_{0,h}$ the Fourier components of the

crystal susceptibility, $\mathbf{u}(\mathbf{r})$ the atomic planes displacements function. Equations (1) are the well known Takagi equations (Takagi, 1969) but without the rescattering term from the diffracted wave to the transmitted one. We consider the most general case of a crystal with an arbitrary variation of the interplanar spacing and the composition, therefore the Fourier components of the crystal susceptibility are coordinate dependent. We restrict ourselves to consideration of the Bragg diffraction geometry only, so the directing sines $\gamma_{0,h}$ and asymmetry factor b are positive.

As the first equation of (1), for the transmitted wave $E_0(\mathbf{r})$, is independent of the second one, its solution can be easily obtained in the form

$$E_0(\mathbf{r}) = E_0(x - \cot\theta_1 z, y, 0)\Phi_0(\mathbf{r}), \qquad (2)$$
$$\Phi_0(\mathbf{r}) = \exp\left\{ i \int_0^z \sigma_0[x + \cot\theta_1(s - z), y, s]\,\mathrm{d}s \right\}.$$

To obtain the analytic solution for the diffracted wave, it is convenient to renormalize its amplitude E_h in the following way:

$$E_h(\mathbf{r}) = \tilde{E}_h(\mathbf{r})\exp(-i\eta z)/\Phi_h(\mathbf{r}), \qquad (3)$$
$$\Phi_h(\mathbf{r}) = \exp\left\{ ib \int_0^z \sigma_0[x - \cot\theta_2(s - z), y, s]\,\mathrm{d}s \right\}.$$

As a result, the second equation (1) takes the form

$$\left(\cot\theta_2 \frac{\partial}{\partial x} - \frac{\partial}{\partial z}\right)\tilde{E}_h(\mathbf{r}) = i\sigma_h(\mathbf{r})\exp\{i[\eta z - \mathbf{hu}(\mathbf{r})]\} \times \Phi(\mathbf{r})E_0(x - \cot\theta_1 z, y, 0), \qquad (4)$$

where $\Phi(\mathbf{r}) = \Phi_0(\mathbf{r})\Phi_h(\mathbf{r})$.

Let us carry out a transition from the field $\tilde{E}_h(\mathbf{r})$ to its Fourier image $\tilde{E}_h(q_x, q_y, z)$, which is:

$$\tilde{E}_h(q_x, q_y, z) = (1/2\pi)\int_{-\infty}^{+\infty}\mathrm{d}x \int_{-\infty}^{+\infty}\mathrm{d}y\,\tilde{E}_h(x, y, z) \times \exp[-i(q_x x + q_y y)]. \qquad (5)$$

As a result, (4) is transformed to the form:

$$\left(iq_x\cot\theta_2 - \frac{\partial}{\partial z}\right)\tilde{E}_h(q_x, q_y, z) = \frac{i}{2\pi}\int_{-\infty}^{+\infty}\mathrm{d}x\int_{-\infty}^{+\infty}\mathrm{d}y\,\sigma_h(\mathbf{r})\exp\{i[\eta z - q_x x - q_y y - \mathbf{hu}(\mathbf{r})]\} \times \Phi(\mathbf{r})E_0(x - \cot\theta_1 z, y, 0). \qquad (6)$$

After replacement,

$$\tilde{E}_h(q_x, q_y, z) = \hat{E}_h(q_x, q_y, z)\exp(iq_x\cot\theta_2 z), \qquad (7)$$

the last equation is written as:

$$-\frac{\partial\hat{E}_h(q_x, q_y, z)}{\delta z} = \frac{i}{2\pi}\int_{-\infty}^{+\infty}\mathrm{d}x\int_{-\infty}^{+\infty}\mathrm{d}y\,\sigma_h(\mathbf{r})\exp\{-i[\mathbf{qr} + \mathbf{hu}(\mathbf{r})]\}\Phi(\mathbf{r})E_0(x - \cot\theta_1 z, y, 0), \qquad (8)$$

where we took into account that $\eta = \cot\theta_2 q_x - q_z$ (see Appendix *A*).

Its solution can be presented as a sum:

$$\hat{E}_h(q_x, q_y, z) = \hat{E}_h(q_x, q_y, z = l) + (i/2\pi)\int_z^l \mathrm{d}z'\int_{-\infty}^{+\infty}\mathrm{d}x\int_{-\infty}^{+\infty}\mathrm{d}y \times \sigma_h(\mathbf{r})\exp\{-i[\mathbf{qr} + \mathbf{hu}(\mathbf{r})]\}\Phi(\mathbf{r}) \times E_0(x - \cot\theta_1 z', y, 0), \qquad (9)$$

where the second term describes the diffracted wave from the surface layer of thickness l and the first one from the underlying crystal (*e.g.* a substrate).

On the entrance surface of the crystal, $E_h(q_x, q_y, z = 0) = \hat{E}_h(q_x, q_y, z = 0)$ and it is written as

$$E_h(q_x, q_y, z = 0) = \hat{E}_h(q_x, q_y, z = l) + (i/2\pi)\int_0^l \mathrm{d}z\int_{-\infty}^{+\infty}\mathrm{d}x\int_{-\infty}^{+\infty}\mathrm{d}y\,\sigma_h(\mathbf{r}) \times \exp\{-i[\mathbf{qr} + \mathbf{hu}(\mathbf{r})]\}\Phi(\mathbf{r})E_0(x - \cot\theta_1 z, y, 0). \qquad (10)$$

Let us consider separately the first term in (10). In accordance with (7) and (3), we have

$$\hat{E}_h(q_x, q_y, z = l) = [E_h(q_x, q_y, z = l) \otimes \Phi_h(q_x, q_y, z = l)]_{q_x, q_y} \times \exp(-iq_z l). \qquad (11)$$

Here the symbol $\otimes$ designates a convolution over q_x and q_y variables:

$$[f(q_x, q_y) \otimes g(q_x, q_y)]_{q_x, q_y} = (1/2\pi)\int_{-\infty}^{+\infty}\mathrm{d}\tau_x\int_{-\infty}^{+\infty}\mathrm{d}\tau_y f(q_x - \tau_x, q_y - \tau_y)g(\tau_x, \tau_y).$$

The solution for $E_h(q_x, q_y, z = l)$ in the case of a semi-infinite uniform crystal (substrate) is straightforward:

$$E_h(q_x, q_y, z = l) = E_0(q_x, q_y, z = l)\exp[-i\mathbf{hu}(z = l)] \times R_\infty(q_x, q_z), R_\infty(q_x, q_z) = \begin{cases} \sigma_h/\xi_1 & \text{if } \Im(\xi) < 0 \\ \sigma_h/\xi_2 & \text{if } \Im(\xi) > 0, \end{cases} \qquad (12)$$

where $\xi = (\tilde{\eta}^2 - 4\sigma_h\sigma_{-h})^{1/2}$, $\xi_{1,2} = \frac{1}{2}(-\tilde{\eta} \pm \xi)$, $\tilde{\eta} = (1 + b)\sigma_0 - q_z - q_x\cot\theta_1$.

By analogy with (11), the explicit expression for $E_0(q_x, q_y, z = l)$ is defined as

$$E_0(q_x, q_y, z = l) = [E_0(q_x, q_y, z = 0)\exp(-iq_x\cot\theta_1 l) \otimes \Phi_0(q_x, q_y, z = l)]_{q_x, q_y}. \qquad (13)$$

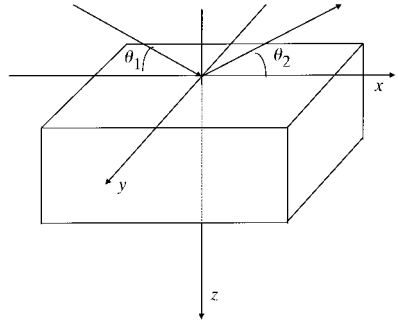

Figure 1
Diffraction geometry used in the theoretical analysis.

In the simplest case when the surface layer is homogeneous in the XY plane, the expressions (11)–(13) are reduced to

$$E_0(q_x, q_y, z = l) = E_0(q_x, q_y, z = 0) \times \exp\left\{i\left[\int_0^l \tilde{\eta}\,\mathrm{d}z - \mathbf{h}\mathbf{u}(z = l)\right]\right\} R_\infty(q_x, q_z), \tag{14}$$

which describes the contribution of the substrate to the scattered wave.

3. Coherent and diffuse scattering

Let us assume that the surface has distortions of the structure (*e.g.* microdefects). The atomic displacement function in this case can be represented as a sum $\mathbf{u}(\mathbf{r}) = \langle\mathbf{u}(\mathbf{r})\rangle + \delta\mathbf{u}(\mathbf{r})$, where the first term describes the averaged displacements and the second one the random deviations from the average. The presence of defects in the surface layer causes the splitting of the reflected intensity in coherent and incoherent (diffuse) components. The general expression for the amplitude of the coherently scattered wave is obtained by statistical averaging of (10) over random displacements. Hereinafter, we suppose that the distorted layer is on the perfect substrate, so that the averaging concerns only the second term in (10). As a result, we get for the coherent amplitude in reciprocal space the following expression:

$$\begin{aligned} E_h^c(\mathbf{q}) &= \langle E_h(\mathbf{q})\rangle \\ &= \hat{E}_h(q_x, q_y, z = l) + (i/2\pi)\int_0^l \mathrm{d}z \int_{-\infty}^{+\infty}\mathrm{d}x \int_{-\infty}^{+\infty}\mathrm{d}y\,\sigma_h(\mathbf{r}) \\ &\quad \times f(\mathbf{r})\Phi(\mathbf{r})\exp\{-i[\mathbf{q}\mathbf{r} + \mathbf{h}\langle\mathbf{u}(\mathbf{r})\rangle]\}E_0(x - \cot\theta_1 z, y, 0), \end{aligned} \tag{15}$$

where $f(\mathbf{r}) = \langle\exp[-i\mathbf{h}\delta\mathbf{u}(\mathbf{r})]\rangle$ is the static Debye–Waller factor.

The distribution of the coherent intensity in the reciprocal space is written as

$$I_h^c(\mathbf{q}) = |E_h^c(\mathbf{q})|^2. \tag{16}$$

The distribution of the diffuse intensity in the reciprocal space is found from the following expression:

$$I_h^d(\mathbf{q}) = \langle E_h(\mathbf{q})E_h^*(\mathbf{q})\rangle - \langle E_h(\mathbf{q})\rangle\langle E_h^*(\mathbf{q})\rangle.$$

With the introduction of the vector $\boldsymbol{\rho} = \mathbf{r} - \mathbf{r}'$, this results in

$$\begin{aligned} I_h^d(\mathbf{q}) = (2\pi)^{-2}&\int_0^l \mathrm{d}z \int_{-z}^{l-z}\mathrm{d}\rho_z \int_{-\infty}^{+\infty}\mathrm{d}x \int_{-\infty}^{+\infty}\mathrm{d}\rho_x \int_{-\infty}^{+\infty}\mathrm{d}y \int_{-\infty}^{+\infty}\mathrm{d}\rho_y \\ &\times \big\{\sigma_h(\mathbf{r} + \boldsymbol{\rho})\sigma_h^*(\mathbf{r})\Phi(\mathbf{r} + \boldsymbol{\rho})\Phi^*(\mathbf{r}) \\ &\times \exp\big(-i\{\mathbf{q}\boldsymbol{\rho} + \mathbf{h}[\langle\mathbf{u}(\mathbf{r} + \boldsymbol{\rho})\rangle - \langle\mathbf{u}(\mathbf{r})\rangle]\}\big) \\ &\times \big(\langle\exp\{-i\mathbf{h}[\delta\mathbf{u}(\mathbf{r} + \boldsymbol{\rho}) - \delta\mathbf{u}(\mathbf{r})]\}\rangle - f(\mathbf{r} + \boldsymbol{\rho})f(\mathbf{r})\big) \\ &\times E_0(x + \rho_x - \cot\theta_l[z + \rho_z], y + \rho_y, 0) \\ &\times E_0^*(x - \cot\theta_l z, y, 0)\big\}. \end{aligned}$$

In the following, we suppose that the linear size of defects is small compared to the distance over which the wave functions present significant variations. This assumption allows us, introducing the correlation function

$$G(\mathbf{r}, \boldsymbol{\rho}) = \big(\langle\exp\{-i\mathbf{h}[\delta\mathbf{u}(\mathbf{r} + \boldsymbol{\rho}) - \delta\mathbf{u}(\mathbf{r})]\}\rangle - f^2(\mathbf{r})\big)/[1 - f^2(\mathbf{r})] \tag{17}$$

and the correlation volume

$$\begin{aligned} \tau(\mathbf{r}, \mathbf{q}) = (2\pi)^{-2}\int_{-\infty}^{+\infty}\mathrm{d}\boldsymbol{\rho}\,G(\mathbf{r}, \boldsymbol{\rho})\exp\big(-i\{\mathbf{q}\boldsymbol{\rho} + \mathbf{h}[\langle\mathbf{u}(\mathbf{r} + \boldsymbol{\rho})\rangle \\ - \langle\mathbf{u}(\mathbf{r})\rangle]\}\big)\exp[i(1 + b)\sigma_0(\mathbf{r})\rho_z], \end{aligned} \tag{18}$$

to present the expression for distribution of the diffusely scattered intensity in reciprocal space in the form

$$\begin{aligned} I_h^d(\mathbf{q}) = \int_0^l \mathrm{d}z \int_{-\infty}^{+\infty}\mathrm{d}x \int_{-\infty}^{+\infty}\mathrm{d}y\,|\sigma_h(\mathbf{r})|^2[1 - f^2(\mathbf{r})]\tau(\mathbf{r}, \mathbf{q}) \\ \times \exp\Big\{-\int_0^z \mu[x + \cot\theta_1(s - z), y, s] + b\mu[x \\ - \cot\theta_2(s - z), y, s]\,\mathrm{d}s\Big\} I_0(x - \cot\theta_1 z, y, 0). \end{aligned} \tag{19}$$

In (19), $\mu = 2\Im(\sigma_0)$ is the photoelectric absorption coefficient.

As a special case of (16) and (19), the expressions for coherently and diffusely scattered intensity for double- and triple-crystal diffractometers may be obtained. The only change to (19) in both cases is the correlation-volume transformation. For the triple-crystal scheme, the expressions must be integrated along the line parallel to the q_y axis and passing through a considered point in the plane of diffraction. As a result, the correlation volume transforms to correlation area

$$\begin{aligned} \tau(\mathbf{r}; q_x, q_z) &= \int_{-\infty}^{+\infty}\mathrm{d}q_y\,\tau(\mathbf{r}, \mathbf{q}) \\ &= (1/2\pi)\int_{-\infty}^{+\infty}\mathrm{d}\rho_z \int_{-\infty}^{+\infty}\mathrm{d}\rho_x\big(\exp[-i(q_z\rho_z + q_x\rho_x)] \\ &\quad \times \exp[i(1 + b)\sigma_0(\mathbf{r})\rho_z] \\ &\quad \times \exp\{-i\mathbf{h}[\langle\mathbf{u}(x + \rho_x, y, z + \rho_z)\rangle \\ &\quad - \langle\mathbf{u}(\mathbf{r})\rangle]G(\mathbf{r}; \rho_x, 0, \rho_z)\big). \end{aligned} \tag{20}$$

With the same integration, the coherent intensity takes the form

$$I_h^c(q_x, q_z) = \int_{-\infty}^{+\infty}\mathrm{d}q_y\,I_h^c(\mathbf{q}) = \int_{-\infty}^{+\infty}\mathrm{d}y\,|E_h^c(q_x, y, q_z)|^2, \tag{21}$$

where $E_h^c(q_x, y, q_z)$ designates the inverse Fourier transformation of $E_h^c(q_x, q_y, q_z)$ over q_y. In particular, the amplitude of the coherent wave from the surface layer becomes

$$\begin{aligned} E_{h,\,\mathrm{layer}}^c(q_x, y, q_z) = [i/(2\pi)^{1/2}]\int_0^l \mathrm{d}z \int_{-\infty}^{+\infty}\mathrm{d}x\,\sigma_h(\mathbf{r})f(\mathbf{r}) \\ \times \exp\{-i[q_z z + q_x x + \mathbf{h}\langle\mathbf{u}(\mathbf{r})\rangle]\} \\ \times \Phi(\mathbf{r})E_0(x - \cot\theta_1 z, y, 0). \end{aligned} \tag{22}$$

The transition to the double-crystal scheme is realized by the integration of (16) and (19) over the plane $-q_z + q_x\cot\theta_2 = \eta$ intersecting the q_z axis at the point $q_z = -\eta$. The correlation volume transforms to correlation length

$$\tau(\mathbf{r},\eta) > = \int_{-\infty}^{+\infty} \mathrm{d}q_x \int_{-\infty}^{+\infty} \mathrm{d}q_y \tau(\mathbf{r}, q_x, q_y, -\eta + q_x \cot\theta_2)$$
$$= \int_{-\infty}^{+\infty} \mathrm{d}\xi \exp(i\eta\xi) \exp[i(1+b)\sigma_0(\mathbf{r})\xi]$$
$$\times \exp\{-i\mathbf{h}[\langle \mathbf{u}(x - \xi\cot\theta_2, y, z+\xi)\rangle - \langle \mathbf{u}(x,y,z)\rangle]\}$$
$$\times G(\mathbf{r}; -\xi\cot\theta_2, 0, \xi). \quad (23)$$

Accordingly, the coherent intensity in this case takes the form

$$I_h^c(\eta) = \int_{-\infty}^{+\infty} \mathrm{d}q_x \int_{-\infty}^{+\infty} \mathrm{d}q_y\, I_h^c(q_x, q_y, -\eta + q_x\cot\theta_2)$$
$$= \int_{-\infty}^{+\infty} \mathrm{d}x \int_{-\infty}^{+\infty} \mathrm{d}y\, |E_h^c(x,y;\eta)|^2, \quad (24)$$

where $E_h^c(x,y;\eta)$ designates the inverse Fourier transformation of $E_h^c(q_x,q_y,q_z)$ over q_y and q_x after replacement $q_z = q_x\cot\theta_2 - \eta$. As an example, the amplitude of the coherent wave from the surface layer takes the form

$$E^c_{h,\,\mathrm{layer}}(x,y;\eta) = \int_0^l \mathrm{d}z\, \sigma_h(x',y,z) f(x',y,z)\Phi(x',y,z)$$
$$\times \exp\{i[\eta z - \mathbf{h}\langle \mathbf{u}(x',y,z)\rangle]\}$$
$$\times E_0(x' - \cot\theta_1 z, y, 0)|_{x'=x-\cot\theta_2 z}. \quad (25)$$

4. Models of defects

Let us consider some simple models of defects that have an explicit form for static factor and correlation volume. In the following, it is convenient to present them in the equivalent form (Bushuev, 1988). In the case of small defect concentration C ($CV_c \ll 1$, V_c is the unit-cell volume), the static factor and the correlation function may be expressed as

$$f = \exp\big[-C\int \mathrm{d}\mathbf{r}\, D(\mathbf{r})\big] \quad (26)$$

and

$$G(\mathbf{r},\boldsymbol{\rho}) = \{C/[1 - f^2(\mathbf{r})]\} \int \mathrm{d}\mathbf{r}'\, D(\mathbf{r}'+\boldsymbol{\rho}) D^*(\mathbf{r}'),$$

where $D(\mathbf{r}) = 1 - \exp[-i\mathbf{h}\delta\mathbf{u}(\mathbf{r})]$.

As a result, the correlation volume is written as follows:

$$\tau(\mathbf{r},\mathbf{q}) = \{C/4\pi^2[1 - f^2(\mathbf{r})]\} \int \mathrm{d}\mathbf{r}'\, \exp(i\mathbf{q}\mathbf{r}') D^*(\mathbf{r}') \exp[i\mathbf{h}\langle \mathbf{u}(\mathbf{r})\rangle]$$
$$\times \int \mathrm{d}\boldsymbol{\rho} \exp[-i\mathbf{q}(\mathbf{r}'+\boldsymbol{\rho})] D(\mathbf{r}'+\boldsymbol{\rho}) \exp[-i\mathbf{h}\langle \mathbf{u}(\mathbf{r}+\boldsymbol{\rho})\rangle].$$

Assuming that within the defect volume the mean displacements are constant (a case of small radius of defects or slowly varying average parameters of the lattice), the difference $\langle \mathbf{u}(\mathbf{r}+\boldsymbol{\rho})\rangle - \langle \mathbf{u}(\mathbf{r})\rangle$ may be replaced by an equivalent difference $\langle \mathbf{u}(\mathbf{r}'+\boldsymbol{\rho})\rangle - \langle \mathbf{u}(\mathbf{r}')\rangle$ that results in the alternative expression for τ:

$$\tau(\mathbf{r},\mathbf{q}) = \{C/4\pi^2[1 - f^2(\mathbf{r})]\} |D(\mathbf{q})|^2, \quad (27)$$

where

$$D(\mathbf{q}) = \int \mathrm{d}\mathbf{r}\, \exp(-i\mathbf{q}\mathbf{r}) D(\mathbf{r}) \exp[-i\mathbf{h}\langle \mathbf{u}(\mathbf{r})\rangle].$$

The calculations of the static factor and the correlation volume for the A–C models are based on expressions (26) and (27). These models describe the spherically symmetrical clusters and the displacement function depends on the distance from the center of the cluster only.

4.1. Spherical amorphous clusters without elastic deformations (model *A*)

The simplest case of the defect crystal is the model of randomly distributed spherical clusters without elastic deformations out of the cluster (Holý, 1982; Bushuev, 1988). The atomic displacement function for the model has the simple form

$$\delta\mathbf{u}(\mathbf{r}) = \begin{cases} \text{arbitrary value}, & |\mathbf{r}| \le R_d \\ 0, & |\mathbf{r}| > R_d, \end{cases}$$

where R_d is the cluster radius.

The corresponding expressions for $D(\mathbf{r})$, f and $D(\mathbf{q})$ are written (see, for instance, Punegov & Pavlov, 1996)

$$D(\mathbf{r}) = \begin{cases} 1, & |\mathbf{r}| \le R_d \\ 0, & |\mathbf{r}| > R_d, \end{cases}$$
$$f = \exp(-CV_{\mathrm{cl}}) \quad (28)$$
$$D(\mathbf{q}) = V_{\mathrm{cl}} 3[\sin(qR_d) - qR_d\cos(qR_d)]/(qR_d)^3, \quad (29)$$

where $V_{\mathrm{cl}} = \frac{4}{3}\pi R_d^3$ is the cluster volume.

4.2. Spherical amorphous clusters with Coulomb-like decreased displacements out of cluster (model *B*)

The strict approach to the problem in the framework of the elasticity theory of an isotropic medium (Teodosiu, 1982) allows the random displacements function of the spherical cluster to be presented in the form

$$\delta\mathbf{u}(\mathbf{r}) = \begin{cases} \text{arbitrary value}, & |\mathbf{r}| \le R_d \\ A\mathbf{r}/r^3, & |\mathbf{r}| > R_d, \end{cases}$$

where A is determined by the inner cluster radius R_d and its strength ε, $A = \varepsilon R_d^3$. The defect strength in its turn is proportional to the crystal volume change owing to a defect insertion into the crystal (Holý & Härtwig, 1988).

With the atomic displacement function, the static factor is written as

$$f = \exp\big(-C(4\pi R_d^3/15)\{3(\sin\tilde{A}/\tilde{A}) + 2\cos\tilde{A} - 4\tilde{A}\sin\tilde{A}$$
$$+ 4(2\pi\tilde{A}^3)^{1/2}\mathrm{Fresnel}C[(2\tilde{A}/\pi)^{1/2}]\}\big), \quad (30)$$

where $\tilde{A} = A|\mathbf{h}|/R_d^2$ and the Fresnel cosine integral is defined as follows:

$$\mathrm{Fresnel}C(x) = \int_0^x \cos[(\pi/2)t^2]\,\mathrm{d}t.$$

Under condition $\varepsilon R_d h \ll 1$, the explicit expressions for $D(\mathbf{r})$ and $D(\mathbf{q})$ take the form

$$D(\mathbf{r}) = \begin{cases} 1, & |\mathbf{r}| \le R_d \\ iA(\mathbf{h}\mathbf{r}/r^3), & |\mathbf{r}| > R_d \end{cases}$$
$$D(\mathbf{q}) = V_{\mathrm{cl}} 3[\sin(qR_d) - qR_d\cos(qR_d)]/(qR_d)^3$$
$$+ \{[4\pi A(\mathbf{h}\cdot\mathbf{q})/q^3][\sin(qR_d)/R_d]\}. \quad (31)$$

The expressions (30) and (31) were derived by Punegov & Pavlov (1996). Deformations out of clusters cause the appearance of the second term in $D(\mathbf{q})$ [compare equations (29) and (31)], which has singularity at the point $\mathbf{q} = 0$. It may be eliminated if we assume that the deformation fields of the clusters are vanishing at some average distance R_I from the center of the cluster. This assumption seems to be correct because of various cluster displacement fields overlapping. The model *C* is based on this assumption.

4.3. Spherical amorphous Coulomb clusters with cut-off displacements (model *C*)

In contrast to model *B*, the displacement function is obtained as

$$\delta\mathbf{u}(\mathbf{r}) = \begin{cases} \text{arbitrary value}, & |\mathbf{r}| < R_d \\ (B\mathbf{r}/r^3) - F\mathbf{r}, & R_d \le |\mathbf{r}| \le R_1 \\ 0, & |\mathbf{r}| > R_1, \end{cases}$$

where $B = AR_1^3/(R_1^3 - R_d^3)$, $F = A/(R_1^3 - R_d^3)$.

With (26), the expression for f is obtained as

$$f = \exp\left(-C\left\{V_{\rm cl} + \frac{4\pi}{|\mathbf{h}|}\int_{R_d}^{R_1} \mathrm{d}r\, r^2 \frac{\sin[|\mathbf{h}|(Br^{-2} - Fr)]}{(Br^{-2} - Fr)}\right\}\right). \quad (32)$$

Under the same condition as for model *B*, *i.e.* $\varepsilon R_d h \ll 1$, we have

$$D(\mathbf{r}) = \begin{cases} 1, & |\mathbf{r}| < R_d \\ i\mathbf{h}\mathbf{r}(B/r^3 - F), & R_d \le |\mathbf{r}| \le R_1 \\ 0, & |\mathbf{r}| > R_1 \end{cases}$$

and

$$\begin{aligned} D(\mathbf{q}) = {} & V_{\rm cl} 3[\sin(qR_d) - qR_d\cos(qR_d)]/(qR_d)^3 \\ & + [4\pi B(\mathbf{h}\cdot\mathbf{q})/q^3][\sin(qR_d)/R_d - \sin(qR_1)/R_1] \\ & + [4\pi F(\mathbf{h}\cdot\mathbf{q})/q^5]\{(qR_1)^2\sin(qR_1) \\ & - 3[\sin(qR_1) - qR_1\cos(qR_1)] - (qR_d)^2\sin(qR_d) \\ & + 3[\sin(qR_d) - qR_d\cos(qR_d)]\}. \end{aligned} \quad (33)$$

4.4. Mosaic crystal model (model *D*)

Following Darwin theory (Darwin, 1922), we assume the crystal consists of a large number of crystalline blocks misoriented at a random angle α and shifted randomly with respect to each other (see Fig. 2). The rotation of a mosaic block by an angle α around the y axis causes a displacement of an arbitrary point (x,y,z) of the block by the vector $\delta\mathbf{u}$, whose components in the plane of diffraction under condition $\alpha \ll 1$ are: $\delta u_x = \alpha z$, $\delta u_z = -\alpha x$. The corresponding atomic displacement function has the form

$$\mathbf{h}\delta\mathbf{u}(x, y, z) = -h(\delta u_x \sin\varphi + \delta u_z \cos\varphi),$$

where φ is an inclination angle of the atomic planes (φ is positive in the case of grazing incidence).

In the following, we assume the relative displacements of the blocks to be comparable with the X-ray wavelength λ. This allows the phase correlation of waves scattered by various blocks to be discarded, *i.e.* to consider the mosaic crystal as an array of independently scattering ideal blocks. For such a crystal model, the static factor is equal to zero ($f = 0$) and the correlation function takes the form

$$G(\boldsymbol{\rho}) = p(\boldsymbol{\rho}) \int_{-\infty}^{+\infty} \mathrm{d}\alpha\, W(\alpha)\exp[iB\alpha(\rho_z\sin\varphi - \rho_x\cos\varphi)],$$

where $B = 4\pi\sin\theta_B/\lambda$; $p(\boldsymbol{\rho})$ is the probability that two points being distant from each other on vector $\boldsymbol{\rho}$ belong to the same block; $W(\alpha)$ is the block misorientation distribution function. Hereinafter, the Gaussian distribution with half-width at half-maximum Δ_m is used, *i.e.*

$$W(\alpha) = [(\ln 2)/\pi]^{1/2}(1/\Delta_m)\exp[-\ln 2(\alpha^2/\Delta_m^2)].$$

As a result, we have

$$G(\boldsymbol{\rho}) = p(\boldsymbol{\rho})\exp\{[-B^2\Delta_m^2(\rho_z\sin\varphi - \rho_x\cos\varphi)^2]/4\ln 2\}. \quad (34)$$

The explicit expression for the correlation volume of a mosaic crystal is obtained by the general expression (18) and dependent on the specific probability function $p(\boldsymbol{\rho})$ determined by the shape and size of the mosaic blocks. We consider the mosaic blocks in the form of a parallelepiped with arrisses l_x, l_y and l_z directed along the coordinate axes. In this case, the probability function takes the form

$$p(\boldsymbol{\rho}) = p_x(\rho_x)p_y(\rho_y)p_z(\rho_z),$$

where

$$p_i(\rho_i) = \begin{cases} 1 - |\rho_i|/l_i, & |\rho_i| \le l_i \\ 0, & \text{otherwise}, \end{cases} \qquad i = x, y, z. \quad (35)$$

5. Instrumental function

In order to take into account the divergence of the beam incident on the sample and the angular reflectivity dependence of the analyzer crystal, the following considerations were examined. Let us assume that the integration over the q_y axis of the intensity $I(q_x,q_y,q_z)$ scattered by the sample is already performed. So we consider the projection of the $I(q_x,q_y,q_z)$ onto the plane (q_x,q_z) of diffraction. Deviation ε of

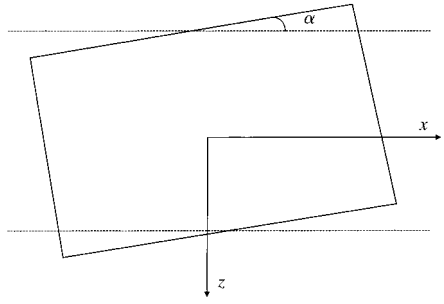

Figure 2
Schematic image of the mosaic block crystal model.

the beam fixed by the analyzer leads to the displacement $k\varepsilon$ ($k = 2\pi/\lambda$ is the wave number) of the considered point (q_x, q_z) in the reciprocal space along the q_ε axis (see Fig. 3). The intensity $\tilde{I}(q_x, q_y)$ after the analyzer is therefore defined by the convolution of the scattered intensity $I(q_x, q_z)$ and the reflectivity angular dependence $R^A(\varepsilon)$ of the analyzer,

$$\tilde{I}(q_x, q_z) = \int_{-\infty}^{+\infty} \mathrm{d}q'_x \, I(q'_x, q_z + \cot\theta_2[q_x - q'_x]) R^A([q_x - q'_x]/k\sin\theta_2),$$

or, after some transformations,

$$\tilde{I}(q_x, q_z) = k\sin\theta_2 \int_{-\infty}^{+\infty} \mathrm{d}\varepsilon \, I(q_x - k\varepsilon\sin\theta_2, q_z + k\varepsilon\cos\theta_2) R^A(\varepsilon).$$

Similarly, the deviation δ of the incident beam onto the sample results in a displacement $k\delta$ of the fixed point in the reciprocal space along the q_δ axis (see Fig. 3). So the convolution of $\tilde{I}(q_x, q_z)$ with the reflectivity angular dependence $R^M(\delta)$ of the monochromator has to be made. This results in the final form of the intensity $I^D(q_x, q_z)$ fixed by the detector in the triple-crystal diffractometer:

$$\begin{aligned} I^D(q_x, q_z) &= \int_{-\infty}^{+\infty} \mathrm{d}\delta \, \tilde{I}(q_x + k\delta\sin\theta_1, q_z + k\delta\cos\theta_1) R^M(\delta) \\ &= k\sin\theta_2 \int_{-\infty}^{+\infty} \mathrm{d}\delta \, R^M(\delta) \int_{-\infty}^{+\infty} \mathrm{d}\varepsilon \, R^A(\varepsilon) I(q_x + k\delta\sin\theta_1 \\ &\quad - k\varepsilon\sin\theta_2, q_z + k\delta\cos\theta_1 + k\varepsilon\cos\theta_2). \end{aligned} \tag{36}$$

6. Results and discussion

Numerical simulations of diffuse intensity distribution (RSM) for the models considered above are presented in Figs. 4–7. The model of spherical amorphous Coulomb clasters with cut-off displacements (model *C*) is the most general among those considered. In the limit of $R_1 = R_d$, it reduces to the model *A* and assuming $R_1 \to \infty$ it transforms to model *B*. Therefore, we restrict ourselves to the analysis of model *C* (Figs. 4 and 5).

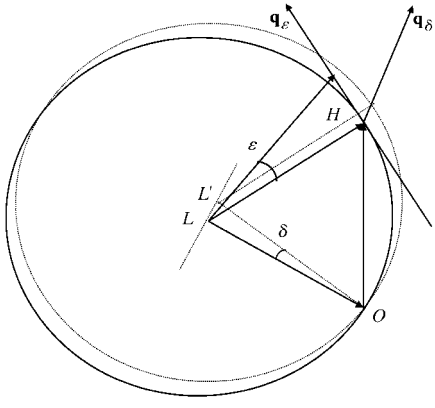

Figure 3
The influence of the instrumental function on the theoretical RSMs formation.

The parameters of the cluster are: inner radius $R_d = 0.1$ μm, external radius $R_1 = 0.232$ μm. The last value corresponds to the defect concentration $C = 10\ \mu\mathrm{m}^{-3}$. Defect strength is varied and equal to $\varepsilon = 10^{-5}$ (Fig. 4*a*), $\varepsilon = 10^{-4}$ (Fig. 4*b*) and $\varepsilon = 10^{-3}$ (Fig. 5*a*). For numerical calculations, the parameters of the 004 reflection of Cu $K\alpha_1$ radiation of a GaAs crystal were used. As follows from Fig. 4(*a*), the diffuse scattering distribution in the case of small defect strength is the same as for model *A*, *i.e.* in the absence of displacement fields out of the cluster. The distribution is spherically symmetrical in this case. Increase in the strength results in the loss of symmetry, shifting of the central maximum along the reciprocal-lattice

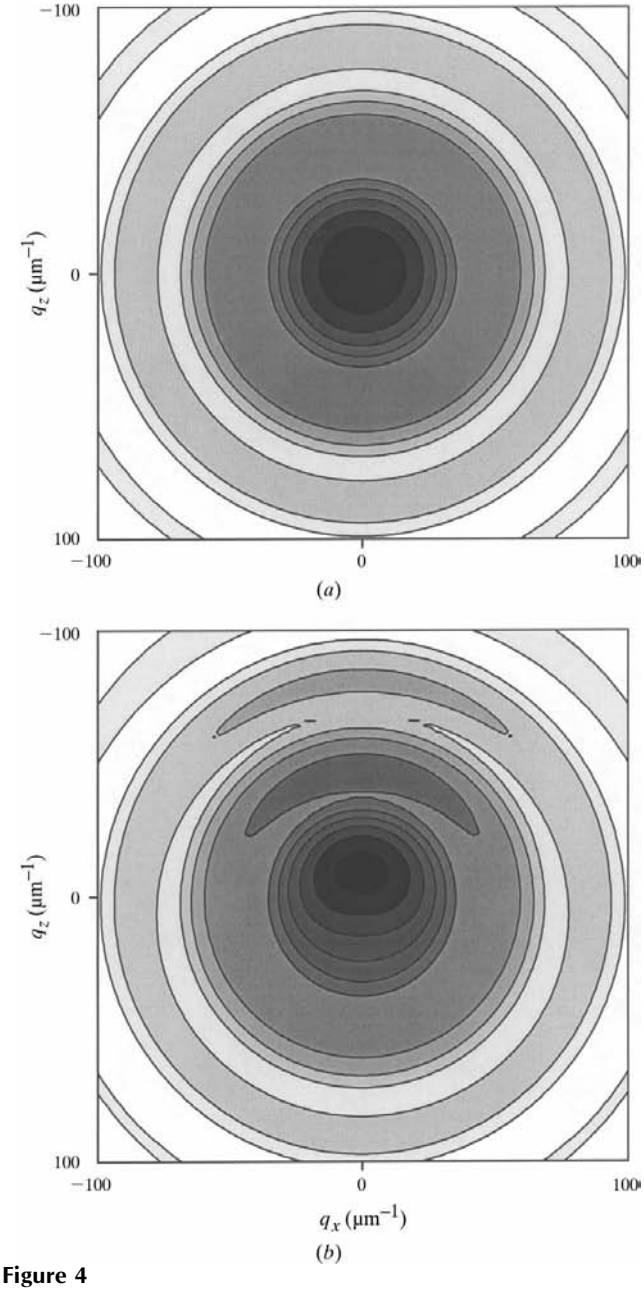

Figure 4
Calculated two-dimensional diffuse-scattering distributions for the model of spherical Coulomb clusters with cut-off displacement fields. For parameters used for the simulation, see text. Defect strength ε is (*a*) 10^{-5} and (*b*) 10^{-4}.

vector (Fig. 4*b*) and its splitting into two peaks at greater values (Fig. 5*a*). The intensity distribution far from the reciprocal-lattice node (not shown on Figs. 4 and 5) remains the same and determined by the structure of the inner part of the cluster. In contrast to Figs. 4 and 5(*a*), which represent intensity distribution integrated over q_y, Fig. 5(*b*) shows the cross section of the distribution in the plane of diffraction. It corresponds to the case of a high horizontally collimated primary beam and a very narrow vertical slit mounted in front of the detector. In comparison with the former case, it has more distinct minima and maxima although the shape of the distribution is kept safe.

Let us consider the intensity distribution from a mosaic crystal (model *D*). Figs. 6 and 7 represent symmetrical and asymmetrical reflection, respectively. The parameters of the imaging crystal used for numerical calculations are the following. We consider the cubic mosaic block with arris $l = 1$ µm, assuming one pair of its planes to be parallel to the diffraction plane. The block misorientation-angle distribution parameter is $\Delta_m = 50''$. The Bragg angle and inclination angle of the scattering atomic planes are $\theta_B = 30^\circ$ and $\varphi = 0^\circ$ for symmetrical reflection and $\theta_B = 50^\circ$ and $\varphi = 40^\circ$ (grazing incidence) for asymmetrical reflection. Figs. 6(*a*) and 7(*a*) are the true two-dimensional distribution while Figs. 6(*b*) and 7(*b*)

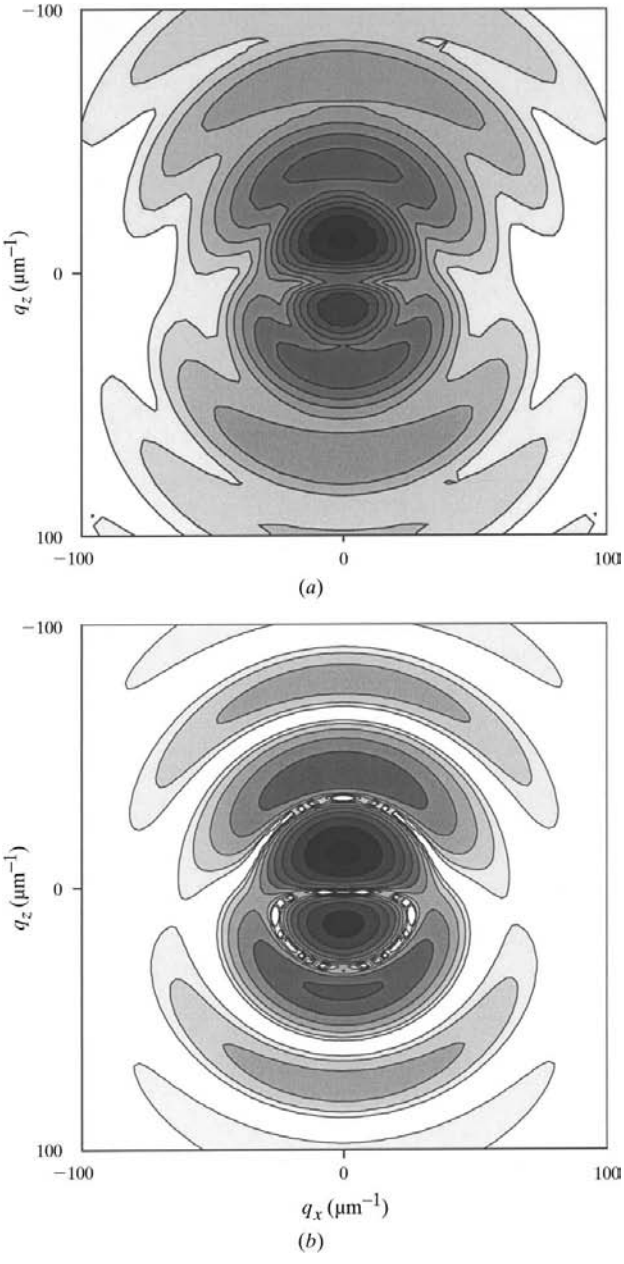

Figure 5
Distribution (*a*) is the same as that in Fig. 4 but with ε equal to 10^{-3} and (*b*) cross section of the corresponding three-dimensional distribution in the plane of diffraction.

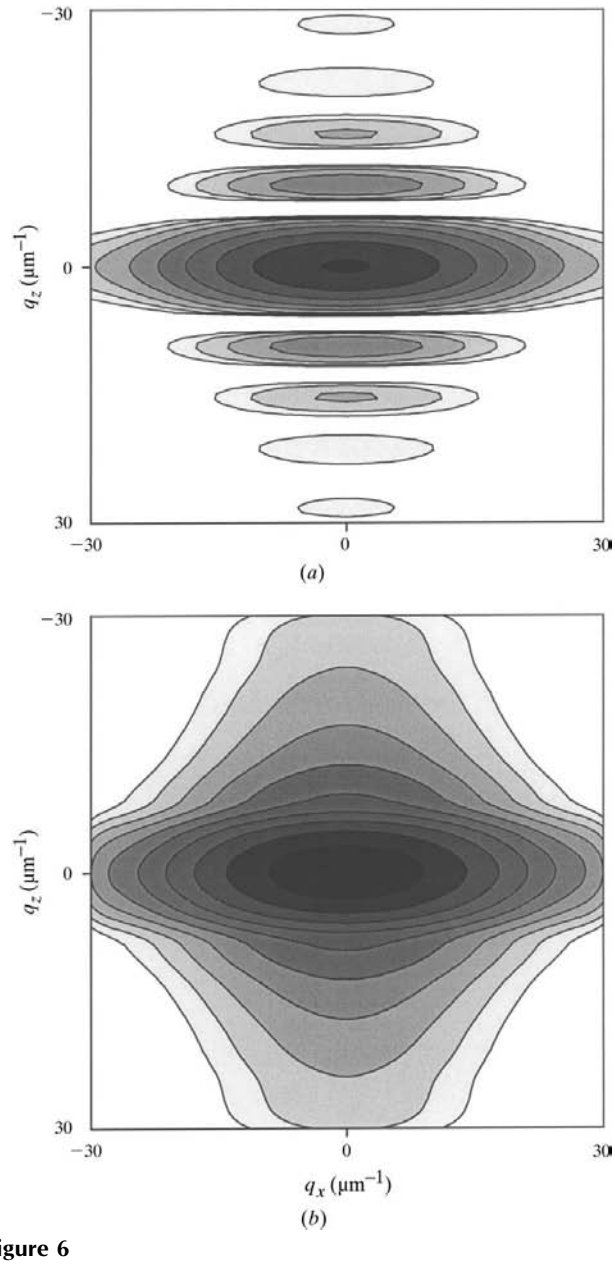

Figure 6
Calculated two-dimensional diffuse-scattering distributions for the mosaic crystal model. Symmetrical reflection. For parameters used for the simulation, see text. The RSM (*a*) before and (*b*) after convolution with the instrumental function are shown.

are the convolution of that with the instrumental function of the triple-crystal diffractometer. As reflectivity angular functions of the monochromator and analyzer, we used Gaussian distributions with half-width at half-maximum ΔM and ΔA, respectively. For the distributions shown in Figs. 6(*b*) and 7(*b*), these parameters are $\Delta M = \Delta A = 10''$.

The most characteristic feature of our mosaic block model is the existence of intensity oscillations in the q_z direction in the case of symmetrical reflection (Fig. 6*a*). Its period coincides with the analogous value for the coherent intensity from the layer of thickness equal to the height of the block. Such behavior is completely determined by the Fourier transform of the $p_z(\xi)$ factor in the probability function. On the contrary, the asymmetrical reflection does not reveal those oscillations (Fig. 7*a*) since, in this case, the intensity in the q_z direction is defined by the Fourier transform of the entire correlation function. For the same reason, these oscillations are absent in the q_x direction for arbitrary reflection (symmetrical or asymmetrical). It is noteworthy that convolution with the instrumental function for relatively large values of ΔM and ΔA smears out the pattern (Figs. 6*b*, 7*b*), with disappearing oscillations. However, for smaller values of ΔM and ΔA (more perfect monochromator and analyzer), in particular $5''$, the oscillations remain.

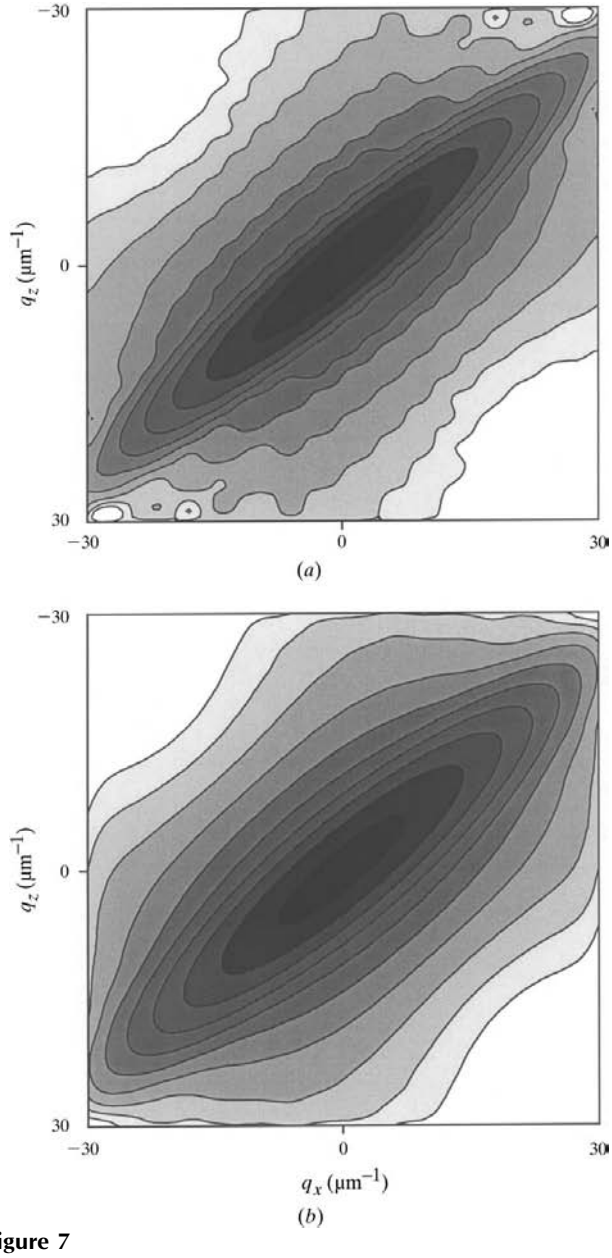

Figure 7
Same as Fig. 6 but for asymmetrical reflection.

7. Conclusions

We have developed a general approach to the kinematical theory of X-ray diffraction in crystals containing random and non-random deformation fields. For simple models of defects, namely spherically symmetrical clusters and mosaic crystals, the numerical diffuse scattering distribution in reciprocal space has been analyzed. Although the main attention was investigation of diffuse scattering, we have obtained general expressions describing the coherent scattering distribution in direct and reciprocal space. The theory will be useful during interpretation of experimental data. Towards this end, the influence of the instrumental function on RSMs was shown.

APPENDIX *A*

The components q_x, q_z of the displacement from the reciprocal point are related to the deviation angles ω and ε of the sample and analyzer by the expressions

$$\begin{aligned} q_x &= h\omega\cos\varphi - k\varepsilon\sin\theta_2 \\ q_z &= -h\omega\sin\varphi - k\varepsilon\cos\theta_2 \end{aligned} \tag{37}$$

or

$$\begin{aligned} \omega &= (q_x\cos\theta_2 - q_z\sin\theta_2)/h\cos\theta_B \\ \varepsilon &= -(q_x\sin\varphi + q_z\cos\varphi)/k\cos\theta_B, \end{aligned} \tag{38}$$

where $k = 2\pi/\lambda$ is the wave number, $h = 2k\sin\theta_B$ is the reciprocal-lattice-vector magnitude.

Let us find the expression for angular parameter η *via* q_x and q_z. As defined,

$$\eta = (2\pi/\lambda\gamma_h)\omega\sin 2\theta_B.$$

Substituting the expression for ω from (37), we obtain

$$\begin{aligned} \eta &= (2\pi/\lambda\sin\theta_2)[(q_x\cos\theta_2 - q_z\sin\theta_2)/h\cos\theta_B]2\sin\theta_B\cos\theta_B \\ &= 2k\sin\theta_B[(\cot\theta_2 q_x - q_z)/h] \\ &= \cot\theta_2 q_x - q_z. \end{aligned}$$

So, for an arbitrary geometry of Bragg diffraction (symmetrical or asymmetrical), the angular parameter η is expressed *via* q_x, q_z as follows:

$$\eta = \cot\theta_2 q_x - q_z. \tag{39}$$

The authors are grateful to the International Association for co-operation of scientists of CIS and Western Europe

counties (grant INTAS-97-31907), to the Russian Federation Education Ministry (grant [1]97-0-7.2-116) and to Syktyvkar State University for financial support.

References

Bushuev, V. A. (1988). Deposited by All-Russian Scientific and Technical Information Institute of the Russian Academy of Sciences, No. 486-B88, pp. 1–55. (In Russian.)

Bushuev, V. A. (1989). *Sov. Phys. Crystallogr.* **34**, 163–167.

Darhuber, A. A., Schittenhelm, P., Holý, V., Stangl, J., Bauer, G. & Abstreiter, G. (1997). *Phys. Rev. B*, **55**, 15652–15663.

Darwin, C. G. (1922). *Philos. Mag.* **43**, 800–829.

Faleev, N., Pavlov, K., Tabuchi, M. & Takeda, Y. (1999). *Jpn J. Appl. Phys.* **38**, 818–821.

Holý, V. (1982). *Phys. Status Solidi B*, **112**, 161–169.

Holý, V., Darhuber, A. A., Bauer, G., Wang, P. D., Song, Y. P., Sotomayor, T. & Holland, M. C. (1995). *Phys. Rev. B*, **52**, 8348–8357.

Holý, V. & Härtwig, J. (1988). *Phys. Status Solidi B*, **145**, 363–372.

Holý, V., Wolf, K., Kastner, M., Stanzl, H. & Gebhardt, W. (1994). *J. Appl. Cryst.* **27**, 551–557.

Iida, A. & Kohra, K. (1979). *Phys. Status Solidi A*, **51**, 533–542.

Kaganer, V. M., Kohler, R., Schmidbauer, M., Opitz, R. & Jenichen, B. (1997). *Phys. Rev. B*, **55**, 1793–1810.

Kato, N. (1980*a*). *Acta Cryst.* A**36**, 763–769.

Kato, N. (1980*b*). *Acta Cryst.* A**36**, 770–778.

Krivoglaz, M. A. (1996). *X-ray and Neutron Diffraction in Nonideal Crystals.* Berlin: Springer-Verlag.

Lomov, A. A., Zaumseil, P. & Winter, U. (1985). *Acta Cryst.* A**41**, 223–227.

Pavlov, K., Faleev, N., Tabuchi, M. & Takeda, Y. (1999). *Jpn J. Appl. Phys.* **38**, Suppl. 38-1, 269–272.

Pavlov, K. M. & Punegov, V. I. (1998*a*). *Acta Cryst.* A**54**, 214–218.

Pavlov, K. M. & Punegov, V. I. (1998*b*). *Acta Cryst.* A**54**, 515.

Pavlov, K. M. & Punegov, V. I. (2000). *Acta Cryst.* A**56**, 227–234.

Punegov, V. I. & Pavlov, K. M. (1996). *Crystallogr. Rep.* **41**, 575–584.

Takagi, S. (1969). *J. Phys. Soc. Jpn*, **26**, 1239–1253.

Teodosiu, C. (1982). *Elastic Models of Crystal Defects*. Bucharest: Editura Academici; Berlin/Heldelberg/New York: Springer-Verlag.

Zaumseil, P. & Winter, U. (1982*a*). *Phys. Status Solidi A*, **70**, 497–505.

Zaumseil, P. & Winter, U. (1982*b*). *Phys. Status Solidi A*, **73**, 455–466.